Available online at www.sciencedirect.com
ScienceDirect
Journal of Solid State Chemistry 179 (2006) 3073–3081
JOURNAL OF SOLID STATE CHEMISTRY
www.elsevier.com/locate/jssc

Rare earth–copper–magnesium compounds $RECu_9Mg_2$ (RE = Y, La–Nd, Sm–Ho, Yb) with ordered $CeNi_3$-type structure

P. Solokha[a,*], V. Pavlyuk[a,c], A. Saccone[b], S. De Negri[b], W. Prochwicz[c], B. Marciniak[c], E. Różycka-Sokołowska[c]

[a]*Department of Inorganic Chemistry, Ivan Franko National University of Lviv, Kyryl and Mefodiy str. 6, 79005 Lviv, Ukraine*
[b]*Dipartimento di Chimica e Chimica Industriale, Sezione di Chimica Inorganica e Metallurgia, Università di Genova, Via Dodecaneso 31, I-16146 Genova, Italy*
[c]*Jan Dlugosz University of Częstochowa, Institute of Chemistry and Environmental Protection, al. Armii Krajowej 13/15, 42200, Częstochowa, Poland*

Received 28 March 2006; received in revised form 23 May 2006; accepted 28 May 2006
Available online 9 June 2006

Abstract

A series of ternary compounds $RECu_9Mg_2$ (RE = Y, La, Ce, Pr, Nd, Sm, Eu, Gd, Tb, Dy, Ho, Yb) have been synthesized via induction melting of elemental metal ingots followed by annealing at 400 °C for 4 weeks. Scanning electron microscopy (SEM) coupled with energy dispersive X-ray spectroscopy (EDXS) was used for examining microstructure and phase composition. These phases crystallize with an ordered version of the binary hexagonal structure type first reported for $CeNi_3$. The crystal structure was solved for $TbCu_9Mg_2$ from single crystal X-ray counter data ($TbCu_9Mg_2$-structure type, $P6_3/mmc$–space group, $hP24$–Pearson symbol, $a = 0.49886\,(7)$ nm, $c = 1.61646\,(3)$ nm, $R_F = 0.0474$ for 190 unique reflections). The Rietveld refinement of the X-ray powder diffraction patterns of $RECu_9Mg_2$ confirmed the same crystal structure for the reported rare earth metals. The unit cell volumes for $RECu_9Mg_2$ smoothly follow the lanthanide contraction. The existence of a $RECu_9Mg_2$ phase was excluded for RE = Er and Tm under the investigated experimental conditions.

Keywords: Intermetallic compounds; Crystal structure; Rare earth metals; Cu-based alloys

1. Introduction

A great number of REM_3 (RE = rare earth, M = transition metal) binary compounds crystallize either in the $NbBe_3$ structure type ($R\bar{3}m$ space group) [1] or in the $CeNi_3$ structure type ($P6_3/mmc$ space group) [2]. These structures are derived from stacking single layers of $CaCu_5$-type units with $MgCu_2$ or $MgZn_2$-type units, respectively. A review on structural and thermodynamic properties of several REM_3 compounds was reported by Latroche and Percheron-Guégan [3].

Several ternary solid solutions form on the basis of REM_3 compounds by partial substitution of the rare earth metal or M with another element: for example Wasylechko et al. [4] studied the effect of gallium on a series of $RENi_3$ compounds (RE = Y, Pr to Lu except Pm and Eu). They established that along the $RENi_{3-x}Ga_x$ compositional line a change from the $NbBe_3$ to the $CeNi_3$ type structure can be observed when increasing the x value.

Moreover, a number of ternary phases are known which adopt the same crystal structure as the REM_3 binaries, in many cases representing ordered derivatives of these structures. An isostructural series of compounds RE_3Ni_8Al (RE = Y, Pr, Nd, Gd–Tm, Lu) which present the Ce_3Co_8Si [5] type structure, derived from the $CeNi_3$ type, was studied by Rykhal et al. [6,7]. Recently in the field of hydrogen storage materials several $RENi_9Mg_2$ (RE = rare earth or Ca) ternary compounds were also investigated, which are reported to crystallize in the $NbBe_3$ structure type [8–11]. On the whole, from the crystal structure point of view, three superstructures related to $NbBe_3$ ($Ca_3Cu_2Al_7$ [12],

*Corresponding author.
E-mail address: solokha_pavlo@yahoo.com (P. Solokha).

0022-4596/$ - see front matter © 2006 Published by Elsevier Inc.
doi:10.1016/j.jssc.2006.05.040

$LaNi_9Mg_2$ and $PrAgAl_2$ [13]) and three related to $CeNi_3$ ($Dy_3Ni_7B_2$ [14], $CeCo_8Si$ and YRh_2Si [15]) are known so far.

In this work results are reported on crystal structure determination and microscopic characterization of a series of $RECu_9Mg_2$ ternary compounds (RE = Y, La–Nd, Sm–Ho, Yb), annealed at 400 °C, crystallizing in a new superstructure related to the $CeNi_3$ structure type. The crystal structure of the ternary compound $TbCu_9Mg_2$ was first successfully determined in the $P6_3/mmc$ space group by the anisotropic approximation of the single crystal method [16]. Later, with the aim to check the existence of ternary compounds with other rare earths, the complete series of ternary alloys with Y, La–Nd, Sm–Yb was prepared and analyzed. The existence of the $CeCu_9Mg_2$ phase was previously reported by Nakawaki et al. [17] who studied the effect of pressure on its electrical resistivity. Nakamori et al. [18–20] have investigated the magnetic, transport and thermodynamic properties for $CeCu_9Mg_2$ and $LaCu_9Mg_2$ compounds.

Table 1
EDXS data of the ternary alloys prepared in this work

RE	Element content in $RECu_9Mg_2$		
	at.%*RE*	at.% Cu	at.% Mg
La	8.6	74.2	17.2
Ce	9.1	74.9	16.0
Pr	8.5	73.2	18.3
Nd	8.6	74.2	17.2
Sm	8.9	75.4	15.7
Eu	8.3	75.1	16.6
Gd	9.2	73.7	17.4
Tb[a]	9.2	74.1	16.7
Dy	9.2	73.5	17.3
Y	9.0	74.2	16.8
Ho	8.9	75.4	15.7
Er	—	—	—
Tm	—	—	—
Yb	8.7	75.2	16.1

The composition accuracy was usually ±0.5 at.%.
[a]The alloy, from which the single crystal has been obtained.

2. Experimental details

2.1. Synthesis

Starting materials for the preparation of the $RECu_9Mg_2$ compounds were the elemental metals, all with nominal purities >99.9 wt.%. Cu was supplied by Aldrich Chemical Company Inc., USA, Mg and rare earth metals by Newmet Koch, Waltham Abbey, England. All samples, each with a

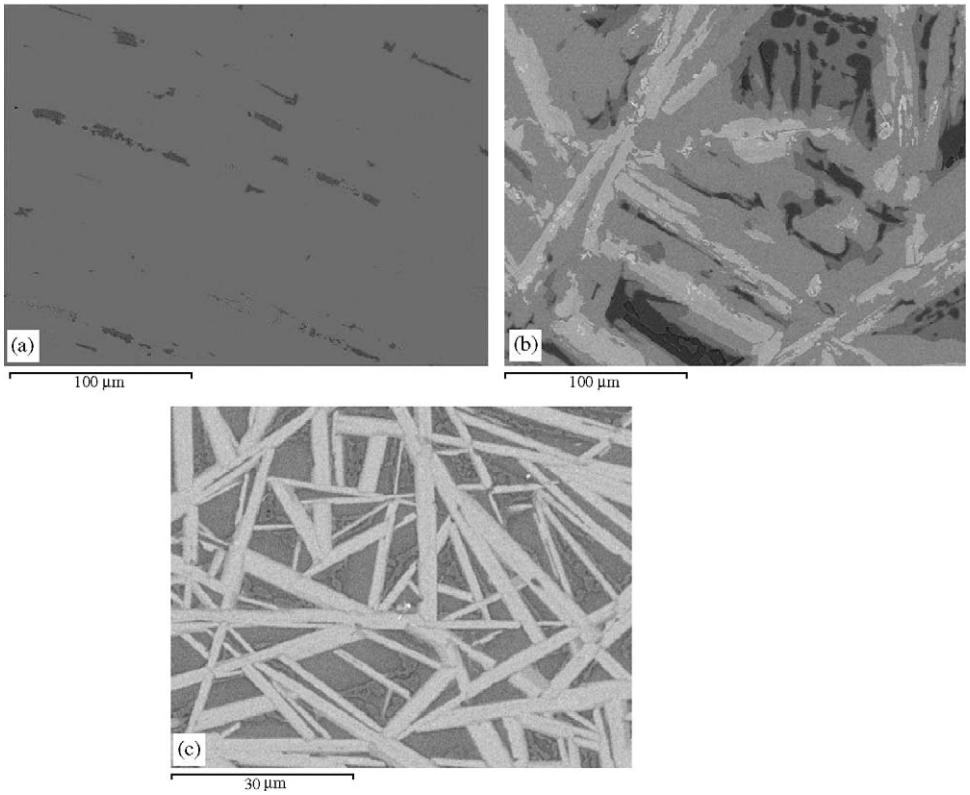

Fig. 1. (a) SEM image (BSE mode) of the microstructure of the Eu-containing sample (main phase: $EuCu_9Mg_2$; gray phase: Cu_2Mg). (b) SEM image (BSE mode) of the microstructure of the Ho-containing sample (bright phase: ~$Ho_{13}Cu_{74}Mg_{13}$; light-gray phase: $HoCu_9Mg_2$; dark-gray phase: ~$Ho_6Cu_{72}Mg_{22}$; dark phase: (Cu)). (c) SEM image (BSE mode) of the microstructure of the Tm-containing sample (bright phase: ~$Tm_{13}Cu_{74}Mg_{13}$; gray phase: Cu_2Mg; dark phase in the eutectic structure: (Cu)).

total weight of about 1 g, were prepared by melting the stoichiometric mixture of the components in an induction furnace under a stream of pure argon, in arc-sealed tantalum crucibles.

The crucibles containing the alloys were then sealed in silica ampoules under argon, annealed in a resistance furnace at 400 °C for 4 weeks, and finally quenched in cold water. After the annealing, the samples could readily be separated from the tantalum crucible. No side-reaction of the samples with the crucible was detected. The samples were stable against air and moisture as compact buttons as well as fine-grained powders. A flat lamina single crystal, exhibiting metallic luster, was isolated by mechanical fragmentation from the annealed sample.

2.2. Optical and electron microscopy microprobe analysis

Sample characterization was carried out by means of light optical microscopy (LOM), scanning electron microscopy (SEM) and energy-dispersive X-ray spectroscopy (EDXS) with the purpose to examine microstructure and phase composition. Smooth surfaces of the specimens were prepared by using SiC papers and diamond pastes down to 1 μm grain size. Quantitative analyses were performed with

Table 2
Crystallographic data for the $TbCu_9Mg_2$ single crystal and experimental details of the structure determination

Empirical formula	$TbCu_9Mg_2$
Structure type	Ordered superstructure to $CeNi_3$
Formula weight (g/mol)	779.40
Crystal system	Hexagonal
Space group	*P*63/*mmc* (No. 194)
Crystal dimensions (μm^3)	$70 \times 60 \times 10$
Unit cell dimensions	
a (nm)	0.49886 (7)
b (nm)	0.49886 (7)
c (nm)	1.61646 (3)
V (nm^3)	0.34838 (10)
Z	2
Calculated density ($D_{calc,}$ $g\,sm^{-3}$)	7.430
Absorption coefficient (μ, mm^{-1})	36.942
Scan mode	ω
Theta range for data collection (deg.)	2.52–27.40
F(0 0 0)	700
Range in *h k l*	$\pm 3,\ \pm 6,\ \pm 20$
Weighing scheme	$1/[\sigma(F_0)^2 + (0.0273 \times P)^2 + 35.75 \times P]$, $P = (\max(F_0^2 + 2F_c^2))/3$
Total no. reflections	380
Independent reflections	190 ($R_{int} = 0.0196$)
Reflections with $I > 2\sigma(I)$	190 ($R_{sigma} = 0.0196$)
Data/parameters	190/19
Goodness-of-fit on F^2	1.294
Final *R* indices [$I > 2\sigma(I)$]	$R_1 = 0.0474$
	$wR_2 = 0.1234$
R indices (all data)	$R_1 = 0.0474$
	$wR_2 = 0.1234$
Extinction coefficient	0.0007(6)
Largest diff. peak and hole	3.734 and $-1.804\,e/Å^3$

Table 3
Atomic coordinates and anisotropic thermal displacement parameters ($nm^2 \times 10$) for the $TbCu_9Mg_2$ single crystal

Atom	Wyckoff position	*x*/*a*	*y*/*b*	*z*/*c*	U_{11}	U_{22}	U_{33}	U_{12}	U_{eq}
Cu_1	2*a*	0	0	0	20 (2)	20 (2)	38 (3)	10 (1)	26 (1)
Cu_2	2*b*	0	0	1/4	16 (2)	16 (2)	36 (3)	8 (1)	23 (1)
Cu_3	2*c*	1/3	2/3	1/4	17 (2)	17 (2)	27 (3)	8 (1)	20 (1)
Tb	2*d*	1/3	2/3	3/4	8 (1)	8 (1)	31 (1)	4 (1)	16 (1)
Mg	4*f*	1/3	2/3	0.5292 (8)	26 (4)	26 (4)	27 (6)	13 (2)	26(1)
Cu_4	12*k*	0.1688 (3)	0.3377 (6)	0.1234 (1)	21 (1)	15 (1)	32 (1)	7 (1)	23 (1)

U_{eq} is defined as one third of the trace of the orthogonalized U_{ij} tensor. The anisotropic displacement factor exponent takes the form: $U_{ij} = -2\pi^2[(h^2a^*)^2U_{11} + \cdots + 2hka^*b^*U_{12}]$. $U_{23} = U_{13} = 0$.

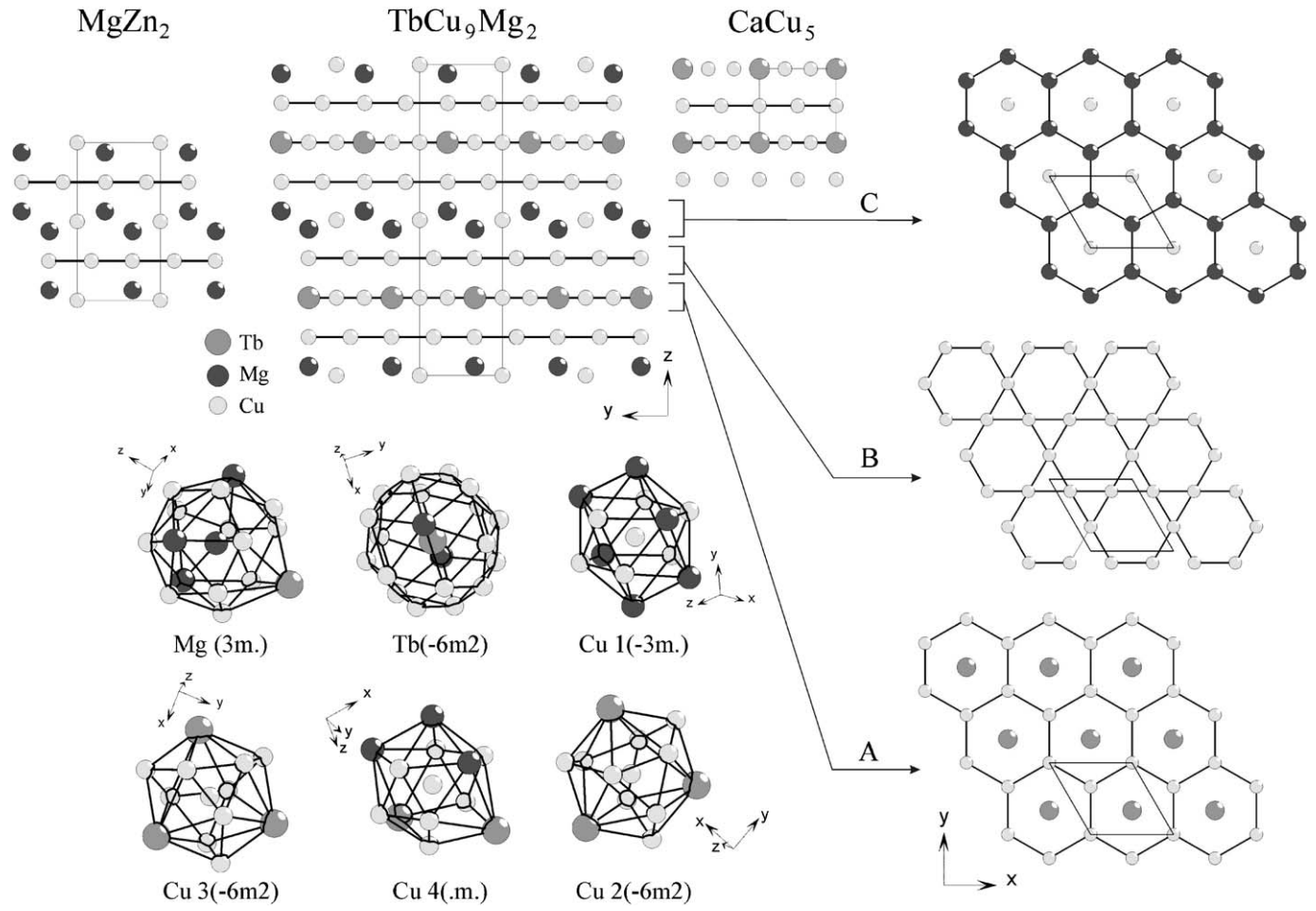

Fig. 2. Crystal structure and coordination polyhedra in the $TbCu_9Mg_2$ structure. In the upper left-hand corner of the figure, the structure is projected onto the z–y plane and relations with $MgZn_2$ and $CaCu_5$ structures are shown. Three atomic layers of this projection are singled out and shown in projections along the hexagonal axis on the right-hand side of the figure. The coordination polyhedra of the six atomic sites are shown in the lower left-hand side and the symmetries of the central atoms are indicated in parentheses.

an acceleration voltage of 20 kV for 50 s. Cobalt standard was used for calibration. X-ray spectra were processed by the software package INCA Energy (Oxford Instruments, Analytical Ltd., Bucks, UK).

2.3. Structure analysis and refinement

Single crystal data were collected at room temperature by using a four-circle diffractometer (*Xcalibur Oxford Diffraction diffractometer*) with CCD detector (graphite monochromatized Mo–$K\alpha$ radiation). Scans were taken in the ω mode. The crystal structure of $TbCu_9Mg_2$ was successfully solved by direct methods and refined using SHELX-97 package programs [21]. The occupancy parameters were refined for this structure to check for deviations from the ideal composition. No significant deviations from the ideal occupancies were found. Hence, in the final refinement cycles of this structure the ideal occupancy parameters were resumed. Data were then corrected for extinction and refined with anisotropic displacement parameters for all atoms. The final difference Fourier syntheses revealed no significant residual peaks. Listings of the observed and calculated structure factors are available.[1] X-ray diffraction on powderized samples was performed by means of the vertical diffractometer *X'Pert* MPD (Philips, Almelo, the Netherlands) with Cu–$K\alpha$ radiation, step mode of scanning, angular range $10^\circ < 2\theta < 100^\circ$ in order to confirm the same structure for other representatives of this isostructural series. Rietveld matrix full profile structure refinements were carried out using the program FULLPROF [22].

3. Results and discussion

3.1. SEM–EDXS characterization

The global compositions measured for the prepared alloys were always very similar to the nominal ones. No

[1]Futher details of the crystal structure investigation can be obtained from the Fachinformationszentrum Karlsruhe, 76344 Eggenstein-Leopoldshafen, Germany, (fax: (49) 7247 808 666; e-mail: crysdata@fiz.karlsruhe.de) on quoting the depository number CSD-416327.

impurity elements were detected in the samples. The results of quantitative analysis on the investigated phases are reported in Table 1; their compositions generally do not differ noticeably from the 1:9:2 stoichiometry.

Most of the prepared samples contain the $RECu_9Mg_2$ as main phase, the amount of secondary phases, either binary or ternary, increasing from light to heavy rare earths. Samples with Eu and Yb are nearly single phase. Generally, the binary phase detected in the samples is Cu_2Mg, solving less than 2 at. % of the rare earth metal. An unknown ternary phase of average composition $RE_6Cu_{72}Mg_{22}$ was detected as a secondary phase in samples containing Ce to Ho except Eu. Moreover a new ternary phase of approximate composition $RE_{13}Cu_{74}Mg_{13}$ was found for RE = Ho, Er, Tm. In samples containing Er and Tm no compounds of the 1:9:2 stoichiometry were found; the existence of this phase was then excluded for these two elements, at least under the experimental conditions adopted in this work. In Fig. 1 the microphotographs of three selected alloys are shown.

3.2. Crystal structure

All the relevant crystallographic data and the experimental details of the structure determination of the $TbCu_9Mg_2$ single crystal are listed in Table 2. The refined positional and thermal displacement parameters are listed in Table 3.

In Fig. 2 the projection of the $TbCu_9Mg_2$ structure onto the z–y plane is presented. This hexagonal structure may be described as an intergrowth of related slabs of the types $CaCu_5$ and $MgZn_2$ having composition $TbCu_5$ and $MgCu_2$. As usual for intermetallics all atoms possess high coordination numbers (CN, Frank–Kasper polyhedra and its derivatives). The Tb–Cu distances of 0.286 and 0.323 nm in hexagonal $TbCu_5$ compare well with the Tb–Cu distances of 0.289 and 0.323 nm in $TbCu_5$ slab of $TbCu_9Mg_2$. The Mg–Mg distance in the structure is a little shorter than in *hcp* magnesium (average Mg–Mg distance of 0.320 nm [23]). Also, the thermal parameters of the Mg positions (see Table 3) with the relatively large CN of 16 are nearly the same when compared to the thermal parameters of the copper positions having CN 12. This indicates that the Mg atoms are strongly bonded to their environments. On the other hand, the terbium atoms have small thermal parameters in spite of their high CN of 20; this reflects their relatively high atomic mass.

This hexagonal structure may be also described as consisting of three kinds of layers, so-called Kagome nets (Fig. 2). The layers of type A and C (6^3-network) are parted

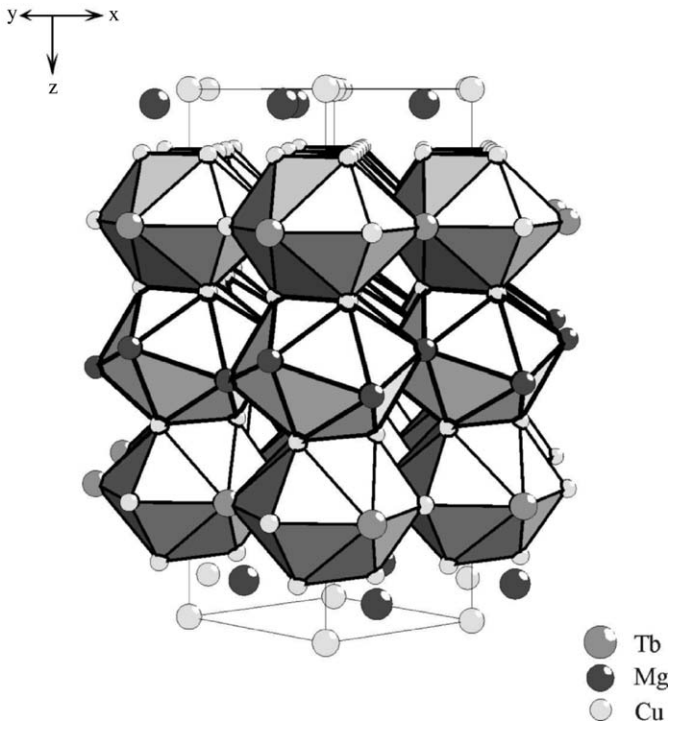

Fig. 3. The perspective view of the arrangement of the icosahedrons and anti-cubooctahedrons in the structure of $TbCu_9Mg_2$.

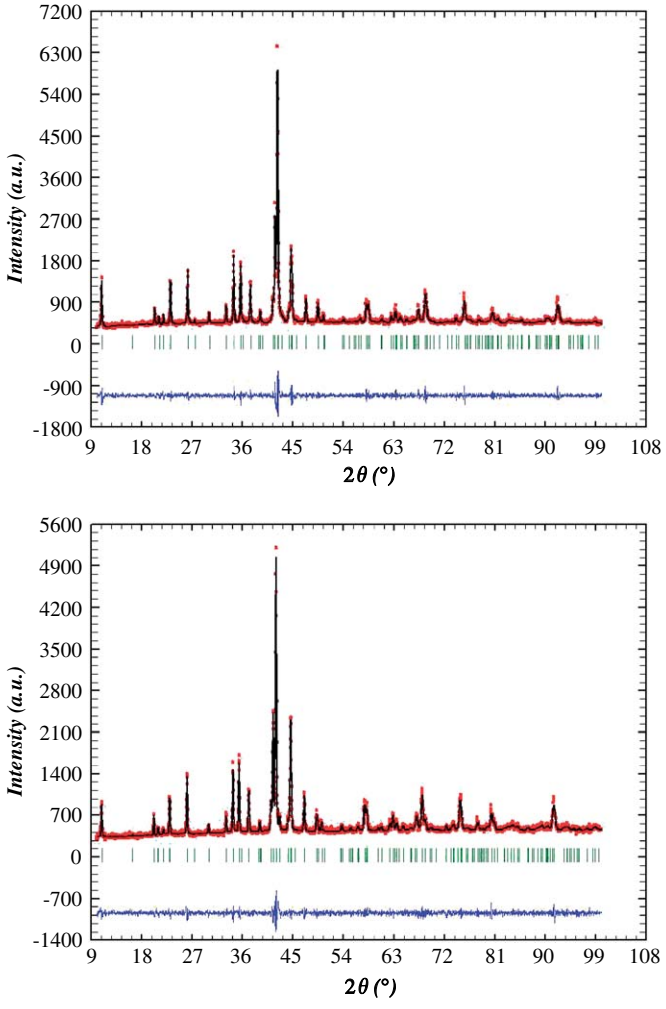

Fig. 4. Experimental and refined XRD patterns for some of the $RECu_9Mg_2$ alloys.

by layers of type B ($3^2 6^2$-network), which consist of only Cu atoms. The layers alternate in the sequence ABCABC. On the other hand, the structure can be completed via the packing of layers of icosahedrons and anti-cubooctahedrons that are close packed by their trigonal edges (Fig. 3).

The XRD powder patterns of the $RECu_9Mg_2$ compounds (RE = Y, La–Nd, Sm–Ho, Yb) obtained in the present investigation match the powder patterns calculated on the basis of the $TbCu_9Mg_2$ structure, by placing the rare earth atoms in the 2*d* site. The reflections of the secondary phases were not observed for the majority of the samples, so that their amount was estimated generally not exceeding 5%. Refined XPD patterns for some $RECu_9Mg_2$ ternary compounds are shown in Fig. 4; the agreement factors for all of them are listed in Table 4. The atomic parameters for the ternary compounds $RECu_9Mg_2$ (RE = Y, La–Nd, Sm–Ho, Yb) are collected in Table 5. The interatomic distances (see Table 6) have appropriate values and do not deviate noticeably from the sum of the atomic radii.

The lattice parameters and the c/a ratios for $RECu_9Mg_2$ compounds are presented in Table 7. The c/a ratio varies between the value 3.2011 for $EuCu_9Mg_2$ and the value 3.2502 for $HoCu_9Mg_2$, a difference of only 1.1%. It can be seen that generally the lattice parameters and cell volumes (Fig. 5) decrease as expected from the lanthanide contraction. Small deviations from the linear decrease may be assigned to small differences in composition. A notable exception is given by the cell parameters of the ternary compounds $EuCu_9Mg_2$ and $YbCu_9Mg_2$, where the europium and ytterbium atoms behave, at least partially, as divalent.

Table 4
Results of Rietveld refinement for $RECu_9Mg_2$ compounds

Compound	Formula weight (g/mol)	Reliability factors					
		R_p	R_{wp}	R_{Bragg}	R_F	R_{exp}	χ^2
YCu_9Mg_2	709.46	0.040	0.056	0.065	0.050	0.023	0.058
$LaCu_9Mg_2$	759.45	0.049	0.075	0.061	0.050	0.033	0.052
$CeCu_9Mg_2$	760.67	0.049	0.066	0.090	0.074	0.039	0.029
$PrCu_9Mg_2$	761.46	0.045	0.066	0.053	0.045	0.030	0.049
$NdCu_9Mg_2$	764.79	0.042	0.060	0.049	0.040	0.028	0.047
$SmCu_9Mg_2$	770.95	0.050	0.067	0.052	0.043	0.043	0.025
$EuCu_9Mg_2$	772.54	0.045	0.059	0.047	0.043	0.044	0.018
$GdCu_9Mg_2$	777.80	0.041	0.056	0.058	0.052	0.032	0.031
$TbCu_9Mg_2$	779.45	0.055	0.071	0.075	0.058	0.048	0.022
$DyCu_9Mg_2$	783.05	0.045	0.060	0.086	0.080	0.034	0.031
$YbCu_9Mg_2$	793.61	0.051	0.068	0.057	0.038	0.037	0.033

The 2θ range of the refined diffraction patterns is 10–100°. The agreement factors for $HoCu_9Mg_2$ are omitted due to the presence of a large quantity of unknown phase in the sample.

Table 5
Atomic parameters of $RECu_9Mg_2$ compounds (RE–Y, La–Nd, Sm–Ho, Yb)

Atom	Wyckoff position	RE	Position *12k*		Position *4f*
			x/a	z/c	z/c
Cu_1	2*a* (0, 0, 0)	Y	0.1660 (3)	0.1220 (1)	0.5290 (4)
		La	0.1686 (8)	0.1194 (2)	0.5281 (6)
Cu_2	2*b* (0, 0, 1/4)	Ce	0.1692 (3)	0.1191 (2)	0.5311 (6)
		Pr	0.1699 (4)	0.1192 (2)	0.5165 (4)
Cu_3	2*c* (1/3, 2/3, 1/4)	Nd	0.1696 (4)	0.1208 (2)	0.5304 (5)
		Sm	0.1683 (5)	0.1211 (2)	0.5309 (6)
RE	2*d* (1/3, 2/3, 3/4)	Eu	0.1685 (4)	0.1193 (2)	0.5304 (6)
		Gd	0.1678 (4)	0.1204 (2)	0.5301 (4)
Mg	4*f* (1/3, 2/3, z)	Tb	0.1649 (6)	0.1238 (3)	0.5372 (9)
		Dy	0.1678 (5)	0.1200 (2)	0.5250 (5)
Cu_4	12*k* (*x*, 2*x*, *z*)	Ho	0.1658 (6)	0.1187 (3)	0.5254 (6)
		Yb	0.1692 (4)	0.1203 (2)	0.5249 (5)

Position of all atoms is standardized by program Structure Tidy [24].

Table 6
Interatomic distances δ (nm) and coordination numbers (CN) of the atoms in some $RECu_9Mg_2$ calculated with the lattice parameters taken from X-ray powder data

	CN	Y	La	Sm	Eu	Tb	Ho	Yb
Pseudo Frank–Kasper								
RE–3Cu_3	20	0.2889	0.2929	0.2902	0.2926	0.2891	0.2880	0.2897
RE–3Cu_2		0.2889	0.2929	0.2902	0.2926	0.2891	0.2800	0.2897
RE–12Cu_4		0.3249	0.3308	0.3269	0.3304	0.3233	0.3274	0.3272
RE–2Mg		0.3580	0.3608	0.3552	0.3561	0.3448	0.3629	0.3641
Icosahedron Frank–Kasper								
Cu_3–6Cu_4	12	0.2530	0.2569	0.2536	0.2567	0.2513	0.2568	0.2537
Cu_3–3Cu_2		0.2889	0.2929	0.2902	0.2926	0.2891	0.2880	0.2897
Cu_3–3*RE*		0.2889	0.2929	0.2902	0.2926	0.2891	0.2880	0.2897
Icosahedron Frank–Kasper								
Cu_2–6Cu_4	12	0.2524	0.2589	0.2553	0.2585	0.2496	0.2561	0.2563
Cu_2–3*RE*		0.2889	0.2929	0.2902	0.2926	0.2891	0.2880	0.2897
Cu_2–3Cu_3		0.2889	0.2929	0.2902	0.2926	0.2891	0.2880	0.2897
Icosahedron Frank–Kasper								
Cu_1–6Cu_4	12	0.2445	0.2442	0.2451	0.2436	0.2463	0.2396	0.2440
Cu_1–6Mg		0.2927	0.2964	0.2945	0.2968	0.2953	0.2909	0.2925
Icosahedron Frank–Kasper								
Cu_4–Cu_1	12	0.2445	0.2442	0.2451	0.2436	0.2463	0.2396	0.2440
Cu_4–2Cu_4		0.2492	0.2506	0.2487	0.2506	0.2478	0.2483	0.2471
Cu_4–Cu_3		0.2530	0.2569	0.2536	0.2562	0.2513	0.2568	0.2537
Cu_4–2Cu_4		0.2511	0.2567	0.2539	0.2564	0.2530	0.2505	0.2548
Cu_4–Cu_2		0.2524	0.2589	0.2553	0.2585	0.2496	0.2561	0.2563
Cu_4–Mg		0.2845	0.2802	0.2854	0.2829	0.2990	0.2746	0.2749
Cu_4–2Mg		0.2920	0.2939	0.2907	0.2915	0.2870	0.2914	0.2946
Cu_4–2*RE*		0.3249	0.3308	0.3269	0.3304	0.3233	0.3274	0.3271
Frank–Kasper								
Mg–3Cu_4	16	0.2845	0.2802	0.2854	0.2829	0.2990	0.2743	0.2749
Mg–3Cu_1		0.2927	0.2939	0.2945	0.2968	0.2953	0.2909	0.2926
Mg–6Cu_4		0.2920	0.2964	0.2907	0.2915	0.2870	0.2915	0.2946
Mg–3Mg		0.3038	0.3068	0.3071	0.3089	0.3133	0.2996	0.3008
Mg–*RE*		0.3580	0.3608	0.3552	0.3561	0.3448	0.3629	0.3641

The interatomic distances found for the other rare earth metals are very similar to those reported.
All distances within the first coordination spheres are listed. Standard deviations are all equal or less than 0.8 pm.

Table 7
Lattice constants of $RECu_9Mg_2$ ternary compounds (*RE*–Y, La–Nd, Sm–Ho, Yb)

Compound	a (nm)	c (nm)	c/a	V (nm^3)	Refs.
YCu_9Mg_2	0.50044 (2)	1.62031 (9)	3.23777	0.35143 (3)	This work
$LaCu_9Mg_2$	0.50733 (2)	1.62633 (9)	3.20566	0.36252 (3)	This work
$CeCu_9Mg_2$[a]	0.5061	1.6260	3.2128	0.3606	[16]
$CeCu_9Mg_2$	0.50558 (2)	1.62439 (10)	3.21292	0.35959 (3)	This work
$PrCu_9Mg_2$	0.50469 (3)	1.62360 (11)	3.21702	0.35816 (4)	This work
$NdCu_9Mg_2$	0.50430 (3)	1.62450 (10)	3.22130	0.35779 (4)	This work
$SmCu_9Mg_2$	0.50270 (2)	1.62204 (10)	3.22666	0.35498 (3)	This work
$EuCu_9Mg_2$	0.50693 (2)	1.62272 (10)	3.20107	0.36114 (3)	This work
$GdCu_9Mg_2$	0.50164 (3)	1.62163 (12)	3.23266	0.35340 (4)	This work
$TbCu_9Mg_2$[a]	0.49886 (15)	1.6165 (5)	3.24039	0.34848 (19)	This work
$TbCu_9Mg_2$	0.50085 (4)	1.62060 (15)	3.23570	0.35208 (6)	This work
$DyCu_9Mg_2$	0.50004 (3)	1.62084 (11)	3.24142	0.35098 (4)	This work
$HoCu_9Mg_2$	0.49889 (8)	1.62149 (15)	3.25020	0.34951 (12)	This work
$YbCu_9Mg_2$	0.50191 (3)	1.61802 (13)	3.22373	0.35299 (5)	This work

[a]Lattice parameters of the single crystals.

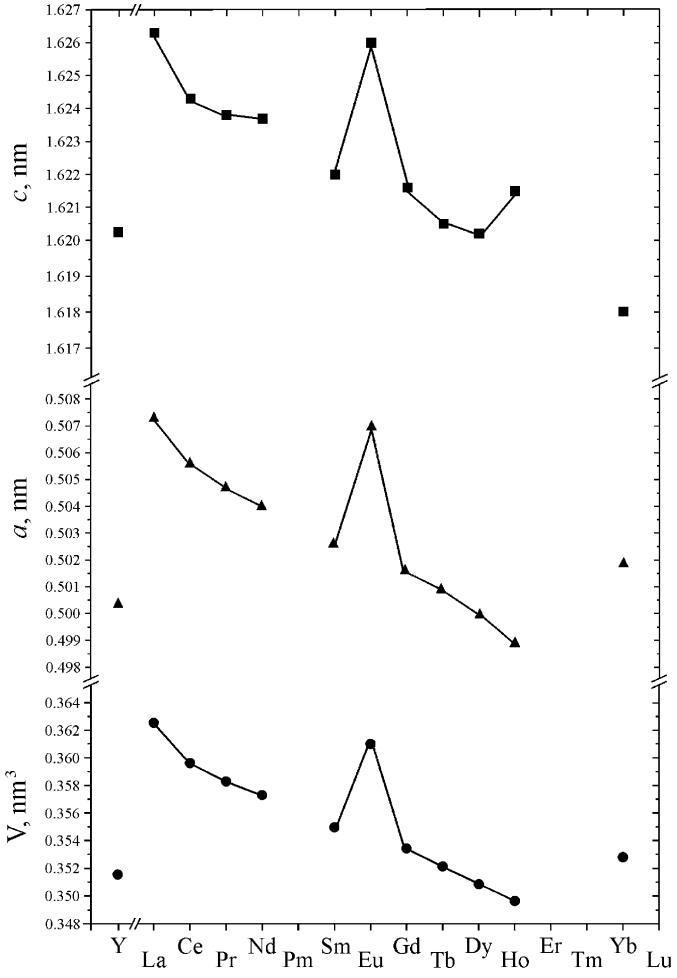

Fig. 5. Plot of the unit cell parameters and volumes of the hexagonal $RECu_9Mg_2$ compounds.

4. Conclusions

The ternary compounds $RECu_9Mg_2$ (RE = Y, La–Nd, Sm–Ho, Yb) were synthesized in the present work and their crystal structure was determined.

All $RECu_9Mg_2$ compounds can be considered as representative of the $R_nM_{5n+2m}R'_m$ structural series which forms by stacking of n RM_5 ($CaCu_5$) and $mR'M_2$ (Laves phase) slabs. For the $RECu_9Mg_2$ $n = 2$, $m = 4$ and this transformation can be expressed by the formula:

$$M_5(RECu_5) + 4R'M_2\ (MgCu_2) = R_2M_{18}R'_4 = 2RECu_9Mg_2.$$

From the crystal structure point of view, the investigated series of compounds represents a new ordered superstructure of the $CeNi_3$ structure type. On the whole, seven superstructures related to $NbBe_3$ and $CeNi_3$ structure types are presently known (see Fig. 6). Each hexagonal superstructure, except Ce_3Co_8Si, has its rhombohedral analog with the same stoichiometry.

Acknowledgments

P. Solokha is grateful to the University of Genova for a research Grant, which gave him the opportunity to start a fruitful collaboration.

References

[1] D.E. Sands, A. Zalkin, O.H. Krikorian, Acta. Crystallogr. 12 (1959) 461–464.
[2] D.T. Cromer, C.E. Olsen, Acta. Crystallogr. 12 (1959) 689–694.
[3] M. Latroche, A. Percheron-Guègan, J. Alloy. Compd. 356&357 (2003) 461–468.
[4] L.O. Wasylechko, Y.N. Grin, A.A. Fedorchuk, J. Alloy. Compd. 219 (1&2) (1995) 222–224.

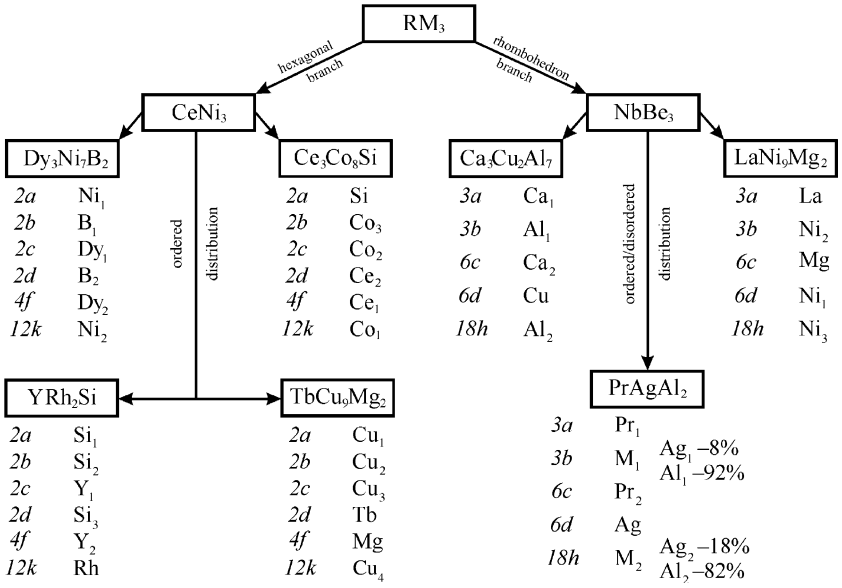

Fig. 6. Ternary derivatives from $CeNi_3$ and $NbBe_3$ structure types.

[5] O.I. Bodak, Visn. L'viv Univ., Ser. Chim. 12 (1971) 22–25.
[6] R.M. Rykhal, O.S. Zarechnjuk, V.M. Mandzyn, Dop. Akad. Nauk Ukr. RSR. A 42 (1980) 77–79.
[7] R.M. Rykhal, O.S. Zarechnjuk, V.S. Protasov, V.A. Romaka, Dop. Akad. Nauk Ukr. RSR B: Geol. Khim. Biol. Nauki. (1982) 41–44.
[8] K. Kadir, I. Uehara, T. Sakaj, J. Alloy. Compd. 257 (1997) 115–121.
[9] K. Kadir, N. Kuriyama, T. Sakaj, I. Uehara, L. Eriksson, J. Alloy. Compd. 284 (1&2) (1999) 145–154.
[10] K. Kadir, T. Sakaj, I. Uehara, J. Alloy. Compd. 287 (1&2) (1999) 264–270.
[11] K. Kadir, T. Sakaj, I. Uehara, J. Alloy. Compd. 302 (1&2) (2000) 112–117.
[12] G. Cordier, E. Czech, H. Ochmann, H. Schafer, J. Less-Common Metals 99 (1984) 173–185.
[13] G. Cordier, E. Czech, G. Dorsam, R. Henseleit, C. Rohr, A. Melner, S. Thies, C. Geibel, J. Less-Common Metals 169 (1991) 55–72.
[14] Yu.B. Kuz'ma, N.F. Chaban, Dop. Akad. Nauk Ukr. RSR. A 42 (1980) 88–91.
[15] L. Paccard, D. Paccard, J. Less-Common Metals 109 (1985) 229–232.
[16] P. Solokha, V. Pavlyuk, A. Saccone, S. De Negri, W. Prochwicz, B. Marciniak, E. Różycka-Sokołowska, in: Ninth International Conference on Crystal Chemistry of Intermetallic Compounds, Lviv (Ukraine), 20–24 September 2005, p. 49.
[17] H. Nakawaki, Y. Inada, R. Asai, M. Yamada, et al., J. Phys.: Condens. Matter. 14 (2002) L305–L311.
[18] Y. Nakamori, M. Ito, H. Fukuda, T. Suzuki, H. Fujii, T. Fujita, Y. Kitano, Physica B 312&313 (2002) 235–236.
[19] M. Ito, K. Asada, Y. Nakamori, H. Fujii, T. Fujita, T. Suzuki, Physica B 329–333 (2003) 482–483.
[20] M. Ito, K. Asada, Y. Nakamori, J. Hori, H. Fujii, F. Nakamura, T. Fujita, T. Suzuki, J. Phys. Soc. Jpn 73 (2004) 2252–2256.
[21] G.M. Sheldrick, SHELXL-97, Program for Crystal Structure Refinement and SHELXS-97, Program for the Solution of Crystal Structures, University of Göettingen, Germany, 1997.
[22] J. Rodriguez-Carvajal, FULLPROF: A Program for Rietveld Refinement and Pattern Matching Analysis, Abstracts of the Satellite Meeting on Powder Diffraction of the XV Congress of the IUCr, Toulouse, France, 1990, p. 127.
[23] G.V. Raynor, Proc. R. Soc. A 174 (1940) 457–471.
[24] E. Parthé, L. Gelato, B. Chabot, M. Penzo, K. Cenzual, R. Gladyshevskii, Typix Standartizated Data and Crystal Chemical Characterization of Inorganic Structure Types, Springer, Berlin, Heidelberg, 1994.